academicJournals

Vol. 11(21), pp. 230-238, 15 November, 2016
DOI: 10.5897/SRE2016.6456
Article Number: 5A94F1F61524
ISSN 1992-2248

http://www.academicjournals.org/SRE

Scientific Research and Essays

Full Length Research Paper

Thermal treatment in air of direct current (DC) magnetron sputtered TiN coatings

Fisnik Aliaj[1], Naim Syla[1]*, Heinrich Oettel[2] and Teuta Dilo[3]

[1]Department of Physics, FMNS, University of Prishtina, Mother Theresa Str.5, KS-10000 Prishtina, Kosovo.
[2]Institute of Materials Science, TU Bergakademie Freiberg, Gustav-Zeuner Str.5, D-09559 Freiberg, Germany.
[3]Department of Physics, FNS, University of Tirana, Boulevard Zogu I, Tirana, Albania.

Received 16 September, 2016; Accepted 5 October, 2016

TiN coatings were deposited onto mirror polished stainless steel substrates by reactive DC magnetron sputtering using a pure Ti target and Ar+N_2 atmosphere. The deposited TiN coatings were thermally treated in ambient air at temperatures ranging from 500 to 700°C for times between 1 and 16 h. The as-deposited and thermally treated coatings were characterized using glow discharge optical emission spectroscopy, x-ray diffraction and scanning electron microscopy. Titanium oxide layers were identified at the surface of thermally treated TiN coatings, which grow according to oxygen diffusion controlled parabolic time law. Phase composition of the oxide layers is found to depend strongly on temperature and exposure time. At low temperatures and shorter exposure times the oxide layers were found to be a mixture of anatase and rutile polymorphs of TiO_2, while at high temperatures and longer exposure times the oxide layers consisted only of the rutile polymorph of TiO_2. The results show that the microstructure of the oxide layers is porous and non-uniform across the oxide layer thickness. The porous microstructure is explained by the accumulation of nitrogen by short-range diffusion and transition into a gaseous state.

Key words: TiN, coating, magnetron sputtering, rutile, thermal treatment, X-ray diffraction (XRD), glow discharge optical emission spectroscopy (GD-OES).

INTRODUCTION

Transition metal nitrides have become universally accepted coatings owing to their exceptional physical and chemical properties, like high hardness, excellent wear resistance, high melting points and chemical stability (Chen et al., 2012; Fateh et al., 2007; Gong et al., 2012; Huang et al., 2006; Mo and Zhu, 2009; Sundgren, 1985; Vaz et al., 2003). Among the transition metal mononitrides, titanium nitride (TiN) is the best-known and -studied coating solution. TiN has been widely used as a wear-resistant hard protective coating on cutting and punching tools, drills, dies and injection molds, and so on (Cunha et al., 2002; Omrani et al., 2012; Zhang and Zhu, 1993). TiN is also very popular as a decorative coating material due to its attractive golden color (Niyomsoan et al., 2002; Nose et al., 2001). Moreover, TiN has found widespread use in many areas of silicon device technology as a diffusion barrier in contact and interconnect metallization schemes (Nicolet, 1978; Shin and Shimogaki, 2004; Yang, 2005), as well as a single phase material for heat-mirror applications (Valkonen et

*Corresponding author. E-mail: naim.syla@uni-pr.edu.

al., 1986). As a hard coating material on cutting tools and machinery parts, TiN coatings are frequently subjected to extreme conditions such as high temperatures, corrosive and oxidizing environments, stresses or a combination of these. Therefore, for TiN coatings subjected to such hostile environments, the understanding of the behavior at elevated temperatures in various oxidizing environments is of increasing importance in applications.

From the thermodynamic point of view, TiN has a favored tendency to replace nitrogen with oxygen when it is exposed to air or oxygen at elevated temperatures; a compound of TiO_2 is formed in the process, which can be understood from the values of heats of formation of -334.9 $kJ \cdot mol^{-1}$ and -916.9 $kJ \cdot mol^{-1}$ for TiN and TiO_2, respectively (Sigurd et al., 1981). TiO_2 exists in three polymorphic forms, namely, rutile (tetragonal), anatase (tetragonal), and brookite (orthorhombic). Rutile is the most thermodynamically stable form, while metastable anatase and brookite transform to rutile upon heating at temperatures above 600 and 700°C, respectively (Wittmer, 1981). Formation of a TiO_2 surface oxide layer when TiN coating is exposed to oxidizing environments at elevated temperatures has been reported by many authors (Chen and Lu, 2005; Hones et al., 2000; Ichimura and Kawana, 1993; Otani and Hofmann, 1996; Tompkins, 1991; Wittmer, 1981). In their studies, the TiO_2 oxide layer was found to grow according to a parabolic rate law with activation energies ranging from 110 to 212 $kJ \cdot mol^{-1}$. Reduced density by pore formation, cracks, and diffusion along grain boundaries in the oxide layer was discussed as the reason for the observed deviations in the activation energy (Chen and Lu, 2005; Ichimura and Kawana, 1993; Otani and Hofmann, 1996).

The aim of this paper was thus to study the behavior of DC magnetron sputtered TiN coatings exposed to elevated temperatures in the range from 500 to 700°C for times between 1 and 16 h, in ambient air. Chemical composition, phase composition and cross-sectional morphology of as-deposited and thermally treated coatings were investigated with Glow Discharge Optical Emission Spectroscopy (GD-OES), X-Ray Diffraction (XRD) and Field-Emission Scanning Electron Microscopy (FE-SEM) techniques, respectively. The main focus was on phase and morphological changes of oxide layers with temperature and exposure time.

MATERIALS AND METHODS

Substrate material

Austenitic stainless steel (DIN 1.4301), which in the following text will be referred to as SS, was used as substrates to deposit the TiN coatings investigated in this work. The substrates were disk shaped with dimensions of $\phi 30 \times 3$ mm. The chemical composition of the substrates as determined with GD-OES is shown in Table 1.

Before loading into the deposition chamber, the disk-shaped substrates were first mechanically grounded and polished to a mirror finish. Next, the substrates were degreased, ultrasonically cleaned for 5 min in a mixture of ethanol and acetone, blown dried with high compressive air and further dried in an oven at ~100°C, and then transferred to the actual deposition environment.

Deposition of the coatings

The TiN coatings were deposited onto mirror-polished SS substrates with reactive DC magnetron sputtering technique by using a Balzers PLS500 apparatus. The pre-cleaned substrates were loaded into the deposition chamber and fixed on a substrate holder which was situated 70 mm above the target. Before deposition, the chamber was evacuated to a base pressure of 2.0×10^{-6} mbar. Next, the substrates were subjected to an RF-etching bias (~13.5 MHz) of 200 W for 5 min in pure Ar plasma in order to remove any traces of surface contamination and the native oxide layer. Coating deposition was then carried out for 60 min in a flowing mixed $Ar+N_2$ atmosphere using a pure Ti target. A bias voltage of -80 V was applied to the substrates and the temperature during deposition was maintained at approximately 400°C.

Thermal treatment in air

After deposition, the TiN coated substrates were subjected to isothermal treatments for various exposure times in ambient atmosphere using a Nabertherm L5 muffle furnace. A type-K thermocouple monitored the temperature of the furnace chamber during isothermal tests. The thermal treatments were performed at different temperatures ranging from 500 up to 700°C for exposure times between 1 and 16 h. The coating samples were first naturally cooled down to temperatures below 100°C in the furnace before moving them out for subsequent analyses.

Characterization techniques

The composition of the as-deposited and thermally treated coatings was determined with GD-OES technique by using an LECO SDP-750 surface depth profiler. GD-OES was also used to estimate the thickness of as-deposited coatings and of oxide layers formed during thermal treatment in air. The phase composition study was conducted by X-ray diffraction (XRD) method in a symmetrical diffraction geometry (θ/2θ scan mode) using a Seifert-FPM RD7 diffractometer equipped with an X-ray tube with Cu anode which was operated at U = 40 kV and I = 30 mA. The cross-sectional morphology was examined by FE-SEM using an LEO 1530 instrument operated at an acceleration voltage of 20 kV.

RESULTS AND DISCUSSION

The thickness of the as-deposited coatings, determined from the GD-OES compositional depth profiles, was found to be in the range between 2.7 and 4.0 μm with an estimated accuracy of ±0.5 μm. The relatively low accuracy for thickness determination by GD-OES is due to interface and surface roughness and the crater-edge effects which are inherent to the GD-OES method (Galindo et al., 2006). The depth at which titanium and iron GD-OES signals intersect each other was used as a measure of the thickness of as-deposited coatings. Figure 1 shows typical GD-OES compositional depth profiles of TiN coatings in the as-deposited state and after thermal treatment in air at indicated temperatures and exposure times. Qualitatively similar GD-OES

Table 1. The chemical composition of stainless steel (SS) substrates used for deposition of TiN coatings (in wt.%). GD-OES measurements were performed on five different specimens, which were cut from the same batch of material, and the average result was taken. The indicated uncertainties are ±2σ.

Cr	Ni	C	N	Mn	P	S	Si	Fe
18.2(1)	9.0(1)	0.025(1)	0.108(5)	1.588(5)	0.039(1)	0.026(1)	0.234(3)	Balance

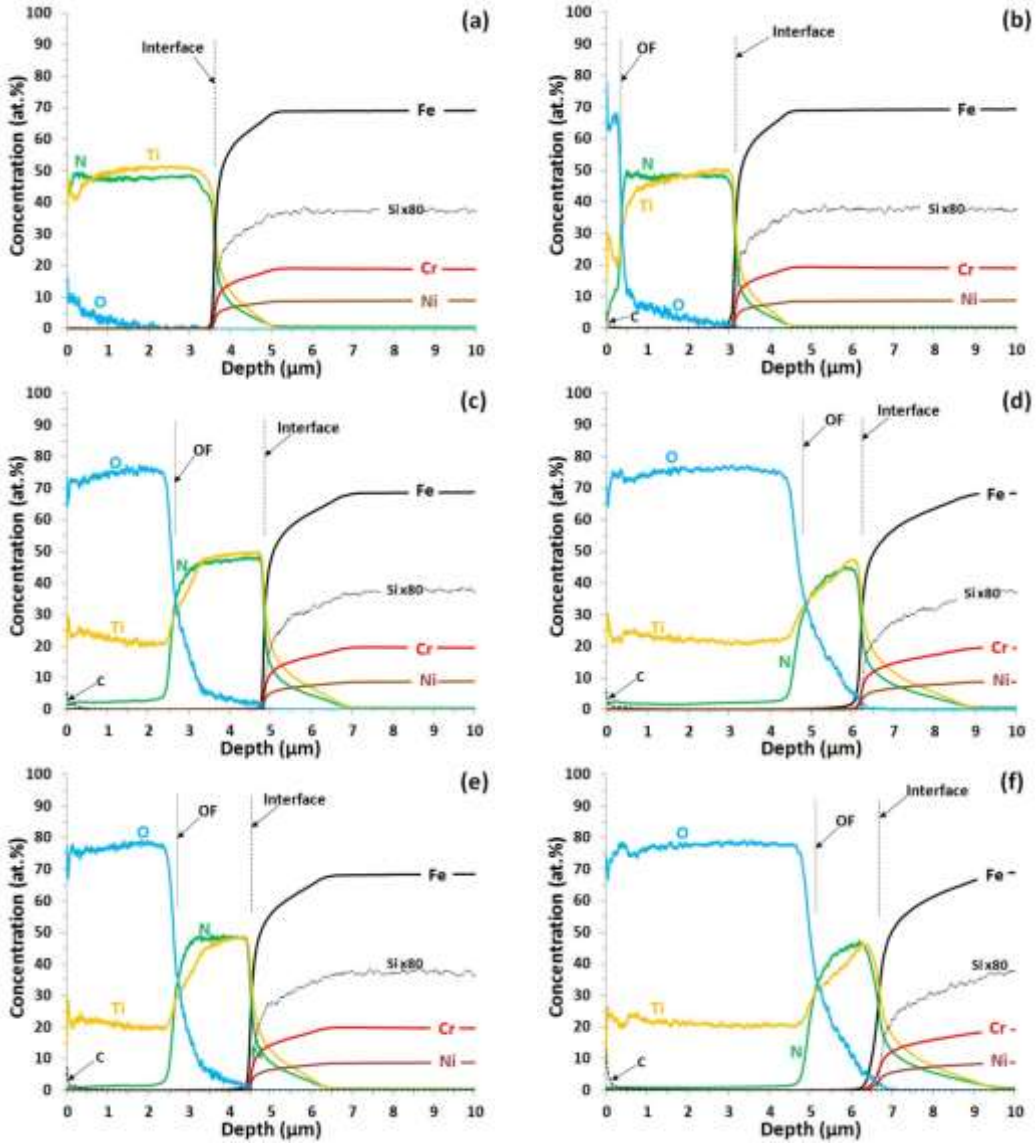

Figure 1. GD-OES compositional depth profiles of TiN coatings in (a) as-deposited condition, and after thermal treatment in air at (b) 500°C for 16 h, (c) 600°C for 16 h, (d) 650°C for 16 h, (e) 700°C for 1 h, and (f) 700°C for 4 h. The Interface dash line indicates the depth from the specimen surface where the iron and titanium concentration profiles intersect each other, which was taken to represent the interface between the coating and the substrate. The OF (oxide front) dot line indicates the depth from the specimen surface where the oxygen concentration drops to 50% of its maximal value, which was taken to represent the thickness of the oxide layer.

profiles were obtained for other temperatures and exposure times. Evidently, the composition of the as-deposited coating is relatively uniform in depth with nitrogen-to-titanium atomic ratio close to the

stoichiometric composition, that is, [N]/[Ti] = 1.0 ± 0.05, which was maintained in the remaining nitride layer of the thermally treated specimens. The as-deposited coatings exhibit a relatively sharp coating/substrate interface. The interface (vertical dash line in Figure 1a) is placed at a depth of the coating where the titanium and iron concentration profiles intersect each other, which for this as-deposited sample is at ~3.6 μm. Also, it is seen that the substrate elements are strictly limited to the substrate and no diffusion of these elements into TiN take place during deposition.

As can be seen in Figure 1, the thermal treatment in air of TiN coatings leads to the formation of an oxide layer the thickness of which increases with temperature and exposure time. The oxide/nitride interface is relatively sharp with practically unaffected nitride layer beneath the oxide layer, a result which is also confirmed by SEM. Studies on TiN oxidation in ambient air (Chen and Lu, 2005; Hones et al., 2000; Ichimura and Kawana, 1993; Otani and Hofmann, 1996; Tompkins, 1991) and oxygen (Milošev et al., 1995; Tompkins, 1991; Wittmer et al., 1981) have shown that an oxide layer composed of TiO_2 grows on top of the TiN coating in a square root of time dependence, implying that the oxidation of TiN is a diffusion limited process. The diffusion of oxygen from the atmosphere through the previously grown oxide layer to the reaction interface, where it progressively replaces nitrogen to form titanium oxides, is discussed as the mechanism governing the TiN oxidation. During oxidation, the replaced nitrogen tends to migrate from the reaction interface through the oxide layer into the atmosphere.

GD-OES profiles show evidence of nitrogen in the oxide layers, which is around 10% at 500°C and less than 1.5% at 700°C. Thermal treatment in air of TiN leads to the release of nitrogen at the oxide/nitride interface. The process responsible for the nitrogen release is believed to be the thermally activated reaction of TiN with oxygen, which is represented as $TiN + O_2 \rightarrow TiO_2 + ½N_2$ with ΔG^o = -582 kJ/mol (Franck et al., 1993). The released nitrogen may accumulate during the thermal treatment and create pores by short-range diffusion and transition into the gaseous state. Obviously, at lower temperatures, the so evolved nitrogen remained still incorporated or trapped in a certain amount within the formed oxide layer. At higher temperatures, however, the nitrogen was almost entirely released into the atmosphere probably due to increased diffusivity constant of nitrogen. A similar nitrogen evolution was reported in the literature for high-temperature annealing in air or oxygen of TiN coatings (Chim et al., 2009; Glaser et al., 2007; Milošev et al., 1995). The formation of porosity by nitrogen evolution during annealing in the air was reported to result in a microstructural degradation of the TiN coatings (Knight, 1990).

GD-OES was very useful for estimating the oxide layer thickness of the thermally treated coatings, which were then used to qualitatively describe the kinetics of the oxide layer growth (to be presented shortly). According to GD-OES depth-profiles, however, the oxygen-to-titanium atomic ratio, [O]/[Ti], in the oxide layers appears to be higher than what was expected. This is particularly the case for the thicker oxide layers, that is, for the coatings thermally treated at higher temperatures and for longer exposure times. The [O]/[Ti] atomic ratio in the thicker oxide layers was found to be ~4 (Figure 1c-f), apparently suggesting that oxide layers corresponding to TiO_4 have developed during thermal treatment in air of TiN coatings. However, XRD measurements show that oxide layers of TiO_2 form during annealing in the air of TiN coatings.

The apparent discrepancy between XRD and GD-OES results was resolved by performing ancillary measurements with electron probe microanalysis with wavelength-dispersive x-ray spectroscopy (EPMA/WDX) across the surface of the TiN coating thermally treated in air at 700 ^oC for 4 h. The reason for choosing this specimen for EPMA measurements is that it exhibits the lowest nitrogen content in the oxide layer, so any possible effect it might have on the outcome of the experiment is minimized. Furthermore, the oxide layer of this specimen is thick enough (~5.1 μm) so as to exclude any possible effect from the underlying TiN layer, which would otherwise give false titanium readings. Before EPMA measurements, the specimen was cleaned ultrasonically for 5 min in ethanol/acetone mixture and was subjected to a drying procedure. The EPMA measurements were then performed at 41 positions randomly distributed across the specimen surface. The results by EPMA show that the oxide layer contains 66 ± 1% oxygen and 34 ± 1% titanium, which is, within the experimental accuracy of the method, very close to that of the stoichiometric TiO_2 compound. This result is in complete agreement with XRD measurements. The apparently higher [O]/[Ti] atomic ratio observed in the GD-OES profiles does not reflect the actual ratio (composition) of the oxide layer. In fact, it appears from the GD-OES results that the level of titanium in the oxide layers was influenced by the level of oxygen displayed in the compositional profile. Some possible explanations of the high oxygen content in oxidized coatings would be a bad conductivity of TiO_2, a high surface roughness or a strange sputtering behavior because of the high porosity of the worn coatings.

The oxidation behavior revealed by GD-OES was confirmed by SEM. Figure 2 shows selected cross-sectional SEM micrographs of TiN coatings in as-deposited state and after thermal treatment in air. As-deposited coating (Figure 2a) is characterized by a dense and columnar microstructure, which is typical for TiN coatings deposited by physical vapor deposition techniques (PVD) techniques (Chen and Lu, 2005; Hones et al., 2000; Ichimura and Kawana, 1993; Knight, 1990; Sabitzer et al., 2015). Evidently, the thermal treatment in air transforms part of the titanium nitride to titanium oxide

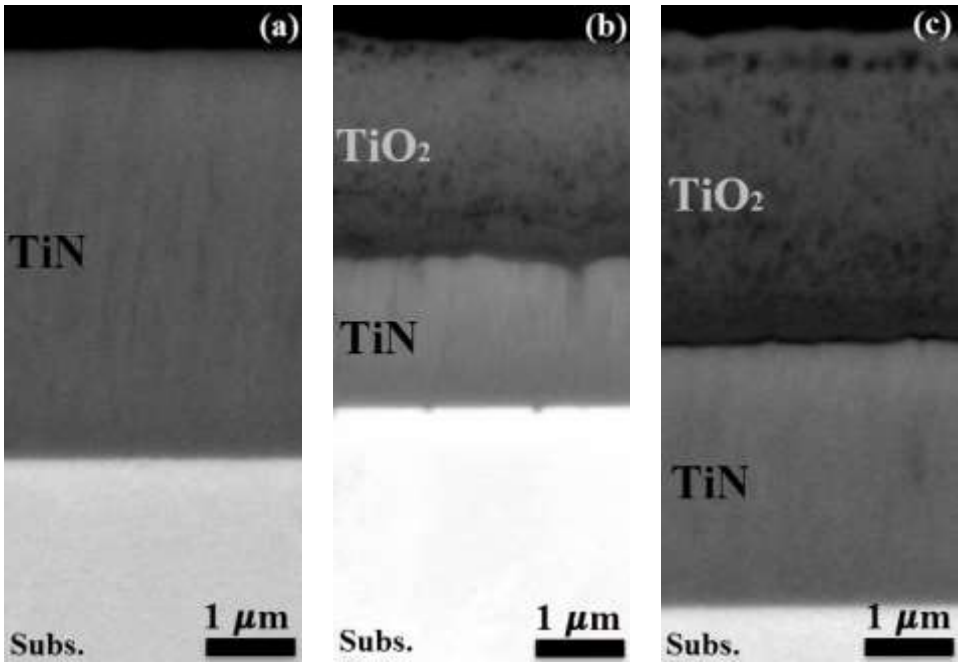

Figure 2. Cross-sectional SEM micrographs of TiN coatings in (a) as-deposited state and after thermal treatment in air (b) at 700 C for 1 h and (c) at 700 C for 2 h.

layer (see Figure 2b-c). A relatively sharp interface is observed between the nitride and oxide region, which is in agreement with GD-OES results previously presented. A similar cross-sectional morphology was reported in the literature for high-temperature annealing in the air of TiN coatings (Chen and Lu, 2005; Feng et al., 2006; Ichimura and Kawana, 1993; Knight, 1990). After thermal treatment in air, the remaining non-reacted TiN layer still exhibits a dense and columnar microstructure, suggesting for a high thermal stability (Sabitzer et al., 2015). The oxide layer is, however, porous and non-uniform across its thickness. Obviously, the pores are much smaller near the oxide/nitride interface and increase in size towards the surface. According to Franck et al. (1993), who studied the surface modification of PVD TiN coatings with concentrated solar energy, the development of non-uniform pore morphology in the oxide layers is a strong indication that the pores are initially nucleated at the oxide/nitride interface and grow substantially during the thermal treatment as the oxide nucleation front moves further inwards.

Figure 3 shows $\theta/2\theta$ XRD patterns of TiN coatings in as-deposited state and after thermal treatment in air at the indicated temperatures and exposure times. As can be seen in the figure, the as-deposited coating is well crystallized in a B1 rocksalt-type cubic structure, c-TiN (PDF-2, 1997). c-TiN and C4 rutile-type tetragonal structure phase, r-TiO_2 (PDF-2, 1997), have been revealed by XRD performed on the surface of the thermally treated coatings, which indicates that TiN transforms to TiO_2 upon thermal treatment in air at elevated temperatures. With increasing the temperature and/or exposure time, the amount of c-TiN transformed to r-TiO_2 increases. Traces of C5 anatase-type tetragonal structure phase, a-TiO_2 (PDF-2, 1997), were also detected up to a certain temperature and exposure time. Figure 4 gives the composition of oxides as a function of temperature (T) and exposure time (t) schematically. It is clearly seen that not only the temperature of heating treatment but also the exposure time influences the composition of the oxide layer. Evidently, a-TiO_2 transforms to r-TiO_2 at T = 600°C for t > 3 h, at T = 650°C for t > 2 h, and at $T \geq$ 700°C for every t. The temperatures for anatase-to-rutile phase transformation observed here for the heating treatment in air of TiN coatings are consistent with the literature (Hanaor and Sorell, 2011; Wittmer et al., 1981).

The XRD profiles of the thermally treated coatings show that the non-reacted underlying nitride layer also exhibits rocksalt-type structure, but the diffraction peaks are slightly shifted to lower diffraction angles relative to the as-deposited state. The shift to lower diffraction angles indicates an increase in the lattice parameter of the TiN phase. The largest increase in the lattice parameter was found to be 0.3%. Different phenomena may account for the observed differences, some of which are described in the following.

i) Relatively sharp interface exists between the oxide and nitride regions of the thermally treated specimens.

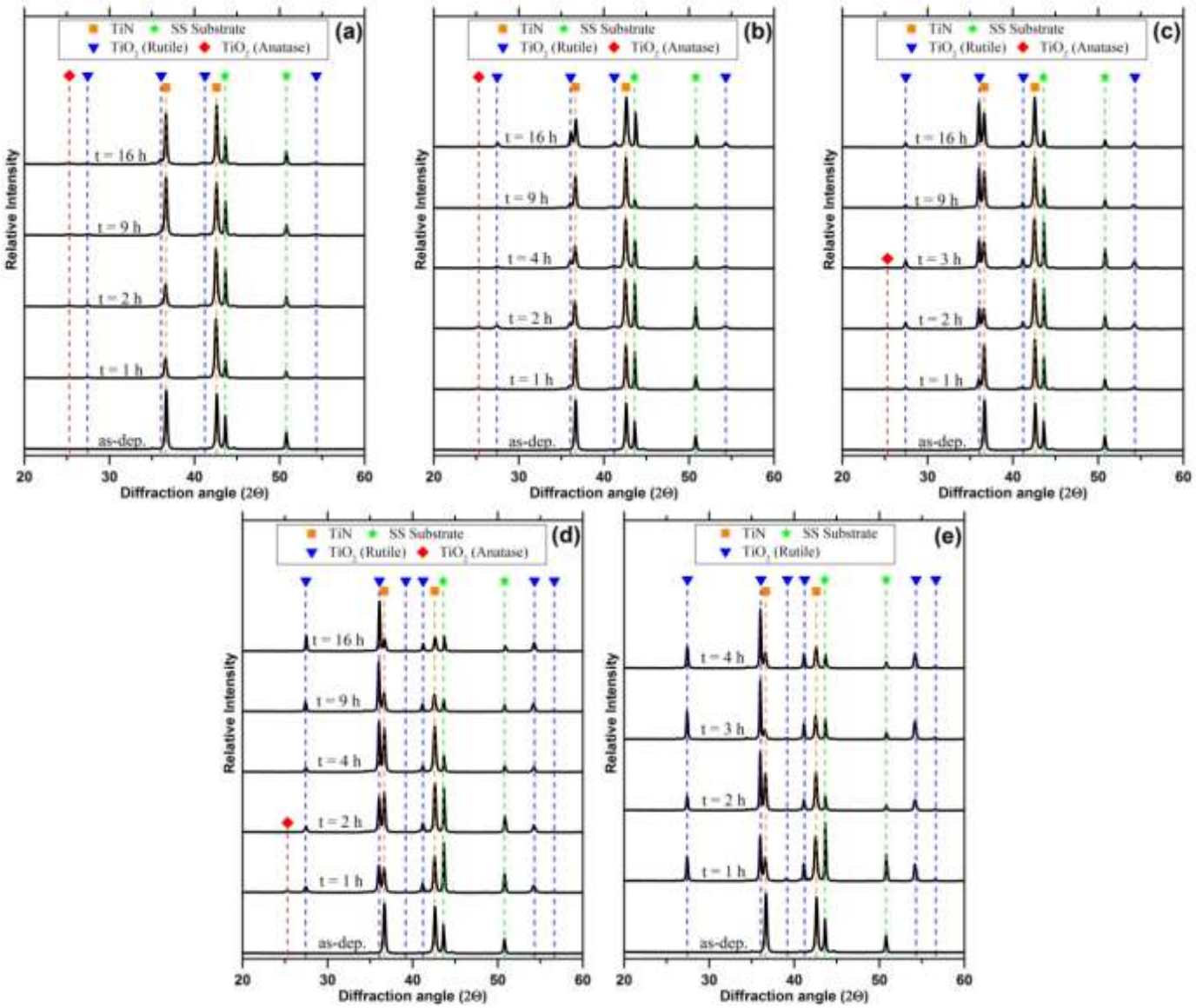

Figure 3. XRD θ/2θ patterns of TiN coatings after thermal treatment at (a) 500, (b) 550, (c) 600, (d) 650, and (e) 700°C at the indicated exposure times. The peaks marked with SS originate from the stainless steel substrate; as-dep. stands for the as-deposited coating. The peak positions for TiN, TiO_2 (rutile), TiO_2 (anatase) and SS phases are taken from the ICDD database (PDF-2, 1997).

However, as seen in the GD-OES profiles (Figure 1), the underlying TiN layer accommodates a certain amount of oxygen, which may be partly responsible for the observed increase in the lattice parameter of the TiN phase. The oxygen in the TiN layer may accommodate at the grain boundaries, at the interstitial sites of the TiN lattice or may partly substitute the N atoms at the normal TiN sites. However, the substitution of N for O atoms is not likely to be the case because the rocksalt-type structured TiO has a shorter lattice parameter (4.17 Å) as compared to rocksalt-type TiN (4.24 Å). This will shrink the average lattice size which is the opposite of what we have observed. Incorporation of oxygen interstitially in the TiN lattice positions should result in an expansion of the lattice, which may partly be accounted for the observed increase in the lattice parameter of TiN. As observed in the GD-OES profiles, the amount of oxygen in the region near the oxide/nitride interface is as much as 30 at.%. However, only a limited amount of the observed oxygen may have dissolved in the interstitial positions of the TiN lattice. Sundgren (1985) have reported an increase in the lattice parameter of 0.2% per every atomic percent of nitrogen for TiN in terms of interstitial incorporation of nitrogen. If it is assumed that the oxygen has the same effect as nitrogen incorporated at interstitial sites, then an oxygen content of ~2.0% will have accounted for the

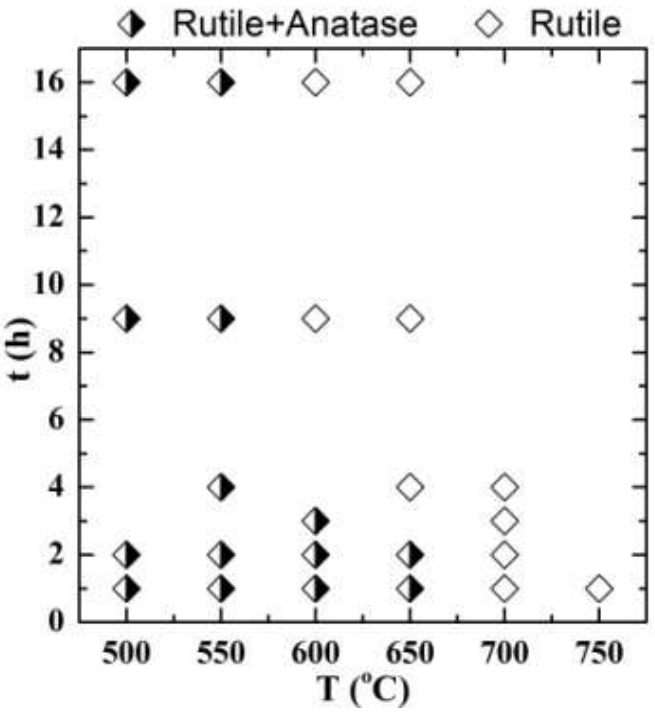

Figure 4. The schematic representation in terms of temperature and time ranges of oxide layer composition after thermal treatment in air of TiN coatings. Half-filled diamonds indicate Rutile + traces of Anatase in oxide layers. Open diamonds indicate only Rutile in oxide layers.

observed increase of 0.3% in the lattice parameter. The rest of the oxygen observed in the TiN layer is believed to be accommodated at the grain boundaries.

ii) The transformation of a part of TiN to TiO_2 as a result of the thermal treatment in air of TiN coatings leads to the generation of stresses in the oxide and underlying nitride layers. These are thermal stresses and growth stresses. Growth stresses, generated as a result of the difference in the molar volumes between the oxide and the nitride which is consumed in its formation, are frequently reported to lead to the formation of cracks at the oxide/nitride interface and to other microstructural degradations (Chen et al., 2012; Ichimura and Kawana, 1993). Even when no stress exists at the reaction temperature, thermal stresses will be generated during cooling because of the difference in thermal expansion coefficient of the oxide, nitride, and substrate. In our case, a description of the sign of the stress in the oxide and nitride layers is rather difficult. However, the shifting of the TiN diffraction peaks to lower diffraction angles is an indication that the underlying TiN layer may be in a compressive stress state. The shifting of the diffraction peaks to lower diffraction angles and the consequent increase in the lattice parameter of the TiN coatings due to compressive residual stress has been reported in the literature (Fateh et al., 2007).

The GD-OES profile of oxygen was used for estimating the oxide layer thickness. Samples of variation of oxygen concentration with depth are shown in Figure 1. The depth at which the oxygen concentration drops to 50% of the maximum value was used as a measure of oxide layer thickness. A plot of the oxide layer thickness as a function of the square root of the period of thermal treatment is shown in Figure 5, for all the investigated temperatures. Evidently, the oxide layer grows according to a parabolic growth law, implying that the oxidation of TiN is diffusion limited. In line with previous investigations by many authors (Chen and Lu, 2005; Hones et al., 2000; Ichimura and Kawana, 1993; Otani and Hofmann, 1996; Wittmer, 1981), the inward diffusion of oxygen through the already grown oxide layer is proposed as a mechanism governing the TiN oxidation.

Conclusions

Thermal treatment of DC magnetron sputtered TiN coatings in ambient air was carried out between 500 and 700°C for exposure times between 1 and 16 h. Based on the results of GD-OES, XRD, and SEM the following conclusions can be made:

i) Thermal treatment in air leads to the formation of a TiO_2 oxide layer on top of the underlying TiN layer. The interface between the oxide and the nitride layers is very sharp. The underlying non-reacted TiN layer appears to have retained the dense and columnar microstructure of the as-deposited coating;
ii) A certain amount of nitrogen released during the thermal treatment remained trapped within the oxide layer, with as much as 10% at 500°C. At the highest temperature investigated, 700°C, any nitrogen released during the thermal treatment was almost entirely diffused out to the atmosphere with less than 1.5% detected in the oxide layer;
iii) The formed oxide layers are porous and non-uniform across thickness, with smaller pores near the oxide/nitride interface and increasing in size towards the oxide surface;
iv) Phase composition of the oxide layer is dependent on temperature and exposure time. At lower temperatures and shorter exposure times the oxide layer consists of a mixture of rutile and anatase polymorphs of TiO_2 (with rutile being the dominating phase), while at higher temperatures and longer exposure times the oxide layer consists only of rutile;
v) The oxide growth was found to follow parabolic time dependence, implying that a diffusion process controls the TiN oxidation. Inward diffusion of oxygen from the atmosphere through the previously grown oxide layer is proposed as the mechanism governing the oxidation.

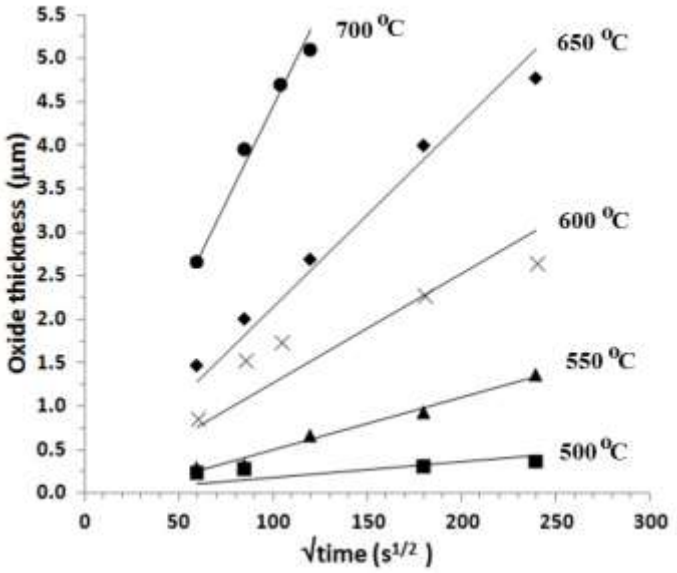

Figure 5. Oxide layer thickness as a function of square root of time at different temperatures. The solid lines represent least-square linear fits.

Conflict of Interests

The authors have not declared any conflict of interests.

ACKNOWLEDGEMENTS

This work was carried out as part of the collaboration between the TU Bergakademie Freiberg and the University of Prishtina within the framework of NMST (Network of Materials Science and Technology). Special thanks goes to the director of the Institute of Materials Science - Prof. D. Rafaja for granting permission to work at the Institute, U. Gubsch for deposition of the coatings, G. Schreiber for XRD analysis, N. Leonhardt for GD-OES measurements, and B. Bleiber for SEM measurements. DAAD is acknowledged for providing financial support.

REFERENCES

Chen HY, Lu FH (2005). Oxidation behaviour of titanium nitride films. J. Vac. Sci. Technol. A23(4):1006-1009.

Chen L, Paulitsch J, Du Y, Mayrhofer PH (2012). Thermal stability and oxidation resistance of Ti-Al-N coatings. Surf. Coat. Technol. 206(11-12):2954-2960.

Chim YC, Ding XZ, Zeng XT, Zhang S (2009). Oxidation resistance of TiN, CrN, TiAlN and CrAlN coatings deposited by lateral rotating cathode arc. Thin Solid Films 517(17):4845-4849.

Cunha L, Andritschky M, Pischow K, Wang Z, Zarychta A, Miranda S, Cunha AM (2002). Performance of chromium nitride and titanium nitride coatings during plastic injection moulding, Surf. Coat. Technol. 153(2-3):160-165.

Fateh N, Fontalvo GA, Gassner G, Mitterer C (2007). Influence of high-temperature oxide formation on the tribological behavior of TiN and VN coatings. Wear 262(9-10):1152-1158.

Feng Ch, Li M, Xin L, Zhu Sh, Wang F (2006). Mechanical properties and oxidation behavior af a graded (Ti,Al)N coating deposited by arc-ion plating. Oxid. Met. 65(5-6):307-327.

Franck M, Blanpain B, Oberländer BC, Celis JP, Roos JR (1993). Surface modification of TiN hard coatings with concentrated solar energy. Sol. Energy Mater Sol. Cells 31(3):401-414.

Galindo RE, Fornies E, Albella JM (2006). Compositional depth profiling analysis of thin and ultrathin multilayer coatings by radio-frequency glow discharge optical emission spectroscopy. Surf. Coat. Technol. 200(22-23):6185-6189.

Glaser A, Surnev S, Netzer FP, Fateh N, Fontalvo GA, Mitterer C (2007). Oxidation of vanadium nitride and titanium nitride coatings. Surf. Sci. 601(4):1153-1159.

Gong C, Zhang J, Yan C, Cheng X, Zhang J, Yu L, Jin Z, Zhang Z (2012). Synthesis and microwave properties of nanosized titanium nitride. J. Mater. Chem. 22(8):3370-3376.

Hanaor DAH, Sorrell CC (2011). Review of the anatase to rutile phase transformation. J. Mater. Sci. 46(4):855-874.

Hones P, Zakri C, Schmid PE, Lévy F, Shojaei OR (2000). Oxidation resistance of protective coatings studied by spectroscopic ellipsometry. Appl. Phys. Lett. 76(22):3194-3196.

Huang JH, Yu KJ, Sit P, Yu GP (2006). Heat treatment of nanocrystalline TiN films deposited by unbalanced magnetron sputtering. Surf. Coat. Technol. 200(14-15):4291-4299.

Ichimura H, Kawana A (1993). High-temperature oxidation of ion-plated TiN and TiAlN films. J. Mater. Res. 8(5):1093-1100.

Knight JC (1990). The effect of annealing on the hardness, interfacial adhesion and wear behaviour of plasma-vapour-deposited TiN coatings on steel. Wear 138(1-2):239-257.

Milošev I, Strehblow H-H, Navinšek B (1995). XPS study of high-temperature oxidation of CrN and TiN hard coatings. Surf. Coat. Technol. 74-75(2):897-902.

Mo JL, Zhu MH (2009). Tribological oxidation behaviour of PVD hard coatings. Tribol. Int. 42(11-12):1758-1764.

Nicolet MA (1978). Diffusion barriers in thin films. Thin Solid Films 52(3):415-443.

Niyomsoan S, Grant W, Olson DL, Mishra B (2002). Variation of color in titanium and zirconium nitride decorative thin films. Thin Solid Films 415(1-2):187-194.

Nose M, Zhou M, Honbo E, Yokota M, Saji S (2001). Colorimetric properties of ZrN and TiN coatings prepared by DC reactive sputtering. Surf. Coat. Technol. 142-144:211-217.

Omrani M, Habibi M, Amrollahi R (2012). Coating of titanium nitride on stainless steel targets by a 4 kJ plasma focus device. J. Fusion Ener. 31(4):401-404.

Otani Y, Hofmann S (1996). High temperature oxidation behaviour of $(Ti_{1-x}Cr_x)N$ coatings, Thin Solid Films 287(1-2):188-192.

PDF-2 (1997). International Centre for Diffraction Data (ICDD). c-TiN 00-038-1420, r-TiO_2 00-021-1276, a-TiO_2 00-021-1272, SS 00-033-0397.

Sabitzer C, Steinkellner C, Koller CM, Polick P, Rauchbauer R, Mayrhofer PH (2015). Diffusion behaviour of C, Cr and Fe in arc evaporated TiN- and CrN- based coatings and their influence on thermal stability and harndess. Surf. Coat. Technol. 275:185-192.

Shin YH, Shimogaki Y (2004). Diffusion barrier property of TiN and TiN/Al/TiN films deposited with FMCVD for Cu interconnection in ULSI. Sci. Technol. Adv. Mater. 5(4):399-405.

Sigurd D, Suni I, Wielunski L, Nicolet MA, Seefeld H (1981). Thermal oxidation of sputtered TiN diffusion barriers. Sol. Cells 5(1):81-86.

Sundgren JE (1985). Structure and properties of TiN coatings (Review Paper). Thin Solid Films 128(1-2):21-44.

Tompkins HG (1991). Oxidation of titanium nitride in room air and in dry O_2. J. Appl. Phys. 70(1):3876-3880.

Valkonen E, Ribbing CG, Sundgren JE (1986). Optical constants of thin TiN films: thickness and preparation effects. Appl. Optics 25(20):3624-3630.

Vaz F, Machado P, Rebouta L, Cerqueira P, Goudeua Ph, Rivière JP, Alves E, Pischow K, de Rijk J (2003). Mechanical characterization of reactively magnetron-sputtered TiN films. Surf. Coat. Technol. 174:375-382.

Wittmer M, Noser N, Melchior H (1981). Oxidation kinetics of TiN thin

films. J. Appl. Phys. 52(11):6659-6664.
Yang LC, Hsu CS, Chen GS, Fu CC, Zuo JM, Lee BQ (2005). Strengthening TiN diffusion barriers for Cu metallization by lightly doping Al. Appl. Phys. Lett. 87(12):1911-1913
Zhang Sh, Zhu W (1993). TiN coating of tools steels: a review, J. Mater. Process. Technol. 39(1-2):165-177.